In *Proc. Allerton Conf. Commun., Contr., Computing,*
(Illinois), Oct. 2000. (invited paper)

A New Class Of Efficient Block-Iterative Interference Cancellation Techniques For Digital Communication Receivers

Albert M. Chan and Gregory W. Wornell

Research Laboratory of Electronics
Massachusetts Institute of Technology
Cambridge, MA 02139
{chanal,gww}@allegro.mit.edu

Abstract

A new and efficient class of nonlinear receivers is introduced for digital communication systems. These "iterated-decision" receivers use optimized multipass algorithms to successively cancel interference from a block of received data and generate symbol decisions whose reliability increases monotonically with each iteration. Two variants of such receivers are discussed: the iterated-decision equalizer and the iterated-decision multiuser detector. Iterated-decision equalizers, designed to equalize intersymbol interference (ISI) channels, asymptotically achieve the performance of maximum-likelihood sequence detection (MLSD), but only have a computational complexity on the order of a linear equalizer (LE). Even more importantly, unlike the decision-feedback equalizer (DFE), iterated-decision equalizers can be readily used in conjunction with error-control coding. Iterated-decision multiuser detectors, designed to cancel multiple-access interference (MAI) in CDMA channels, asymptotically achieve the performance of the optimum multiuser detector in uncoded systems, but only have a computational complexity on the order of a decorrelating detector or a linear minimum mean-square error (MMSE) multiuser detector.

1 Introduction

Over the last several decades, a variety of equalization techniques have been proposed for use on intersymbol interference (ISI) channels. Linear equalizers (LE) are attractive from a complexity perspective, but often suffer from excessive noise enhancement. Maximum-likelihood sequence detection (MLSD) is an asymptotically optimum receiver in terms of bit-error rate performance, but its high complexity has invariably precluded its use in practice. Decision-feedback equalizers (DFE) [1] are a widely used compromise, retaining a complexity comparable to the LE, but incurring much less noise enhancement. However, DFEs still have some serious shortcomings. First, decisions made at the slicer can only be fed back to improve future decisions due to the sequential way in which the receiver processes data. Thus, only postcursor ISI can be subtracted, so even if ideal postcursor

This work has been supported in part by NSF under Grant No. CCR-9979363, Qualcomm, Inc, and Sanders, a Lockheed-Martin Company.

ISI cancellation is assumed, the performance of the DFE is still limited by possible residual precursor ISI and noise enhancement. Second, and even more importantly, the sequential structure of the DFE makes it essentially incompatible for use in conjunction with error-control coding (on channels not known at the transmitter, as is the case of interest in this paper). As a result, use of the DFE has been largely restricted to uncoded systems.

In parallel to these developments, a variety of multiuser detectors have been proposed for CDMA channels over the last decade and a half as solutions to the problem of mitigating multiple-access interference (MAI) [2]. Given the close coupling between the problems of suppressing ISI and MAI, there are, not surprisingly, close relationships between corresponding solutions to these problems. For example, decorrelating detectors and linear minimum mean-square error (MMSE) multiuser detectors—the counterparts of zero-forcing and linear MMSE equalizers are attractive from a complexity perspective, but suffer from noise enhancement. Optimum maximum likelihood (ML) multiuser detection, while superior in performance, is not a practical option because of its high complexity.

In this paper, we introduce a class of remarkably efficient multipass receivers that is a particularly attractive alternative to all these conventional equalizers and detectors. Specifically, in Section 2 we describe the iterated-decision equalizer, and in Section 3 we describe the corresponding multiuser iterated-decision detector. In particular, we show that these new receivers achieve asymptotically optimum performance while retaining low complexity.

2 The Iterated-Decision Equalizer

In the discrete-time baseband model of the pulse amplitude modulation (PAM) communication system we consider, the transmitted data is a white M-ary phase-shift keying (PSK) stream of coded or uncoded symbols $x[n]$, each with energy $\mathcal{E}_s$. The symbols $x[n]$ are corrupted by a convolution with the channel impulse response, $a[n]$, and by additive noise, $w[n]$, to produce the received symbols[1] $r[n] = a[n] * x[n] + w[n]$. The noise $w[n]$ is a zero-mean, complex-valued, circularly symmetric, stationary, white Gaussian noise sequence with variance $\mathcal{N}_0$ that is independent of $x[n]$. (To simplify the exposition, we focus on symbol-spaced equalization. However, the fractionally spaced generalizations required in practice follow in a straightforward manner, as developed in [4].)

Also, as increasingly aggressive data rates are pursued in wideband systems to meet escalating traffic requirements, ISI becomes increasingly severe. Accordingly, in this paper we pay special attention to the performance and properties of the equalizers in this regime. For the purposes of analysis, a convenient severe-ISI channel model we will exploit is one in which $a[n]$ is a finite impulse response (FIR) filter of length L, where L is large and the taps are mutually independent, zero-mean, complex-valued, circularly symmetric Gaussian random variables with variance σ_a^2. The channel taps $a[n]$ are also independent of the data $x[n]$ and the noise $w[n]$. Note that this is also a good channel model for many wireless systems employing transmitter antenna diversity in the form of linear space-time coding [5].

We begin by focussing on the case in which the receiver has exact knowledge of $a[n]$ in order to develop the basic theory and fundamental limits. In Section 2.1, we consider

[1] The symbol $*$ denotes the convolution operation.

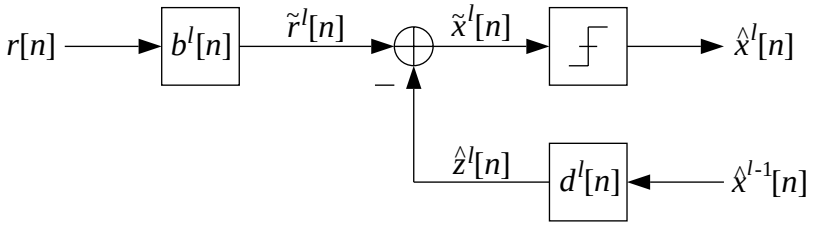

Figure 1: Iterated-decision equalizer structure.

the case of practical interest in which the receiver does not have *a priori* knowledge of the channel, and develop a corresponding adaptive equalizer. We emphasize that in both cases, we restrict our attention to transmitters that have no knowledge of the channel, which is the usual case for reasonably rapidly time-varying channels.

The iterated-decision equalizer we now develop processes the received data in a block-iterative fashion [4, 3]. Specifically, during each iteration or "pass," a linear filter is applied to all the received data, and tentative decisions made in the previous iteration are then used to construct and subtract out an estimate of the ISI. The resulting ISI-reduced data is then passed on to a slicer, which makes a new set of tentative decisions. With each successive iteration, increasingly refined hard decisions are generated using this strategy.

The detailed structure of the iterated-decision equalizer is depicted in Fig. 1.[2]

The parameters of all systems and signals associated with the lth pass are denoted using the superscript l. On the lth pass of the equalizer where $l = 1, 2, 3, \ldots$, the received data $r[n]$ is first processed by a linear filter $b^l[n]$, producing the sequence $\tilde{r}^l[n] = b^l[n] * r[n]$. Next, an appropriately constructed estimate $\hat{z}^l[n]$ of the ISI is subtracted from $\tilde{r}^l[n]$ to produce $\tilde{x}^l[n]$, i.e., $\tilde{x}^l[n] = \tilde{r}^l[n] - \hat{z}^l[n]$, where $\hat{z}^l[n] = d^l[n] * \hat{x}^{l-1}[n]$. Since $\hat{z}^l[n]$ is intended to be some kind of ISI estimate, we impose the constraint that the zero-delay tap of $d^l[n]$ be zero or, equivalently, that $\frac{1}{2\pi}\int_{-\pi}^{\pi} D^l(\omega)d\omega = 0$. The slicer then generates the hard decisions $\hat{x}^l[n]$ from $\tilde{x}^l[n]$ using a minimum-distance rule.

Analogous to counterparts in [5] and [6], we have that when $x[n]$ and $\hat{x}^{l-1}[n]$ are sequences of zero-mean uncorrelated symbols, each with energy $\mathcal{E}_s$, such that their normalized correlation is of the form $E[x^*[n] \cdot \hat{x}^{l-1}[k]]/\mathcal{E}_s \approx \rho^{l-1}\delta[n-k]$, then the slicer input at each iteration can be expressed as

$$\tilde{x}^l[n] \approx E[AB^l]x[n] + v^l[n] \tag{1}$$

where $A(\omega)$ and $B^l(\omega)$ are the frequency responses of $a[n]$ and $b^l[n]$ respectively, where $v^l[n]$ is a complex-valued, marginally Gaussian, zero-mean white noise sequence, uncorrelated with the input symbol stream $x[n]$ and whose variance is a function of $B^l(\omega)$ and $D^l(\omega)$, and where the accuracy of the approximation in (1) increases with the length L of the impulse response $a[n]$.

The second-order model (1) turns out to be a useful one for analyzing and optimizing the performance of the iterated-decision equalizer. In particular, the signal-to-interference+noise ratio (SINR) at the slicer input during each pass, defined as $\gamma^l =$

[2] As developed in [3, 4], for coded systems, it suffices to replace the slicer in Fig. 1 with the associated decoder, and to re-encode the previous iteration's decisions $\hat{x}^{l-1}[n]$ before they are input to $d^l[n]$. Note that for DFE's, this kind of integration of decoding with equalization is not possible due to causality constraints.

$\mathcal{E}_s|E[AB^l]|^2/\text{var } v^l[n]$, achieves a maximum value of

$$\gamma^l = \left(\frac{1}{1 - \mathcal{E}_s(1-(\rho^{l-1})^2) E\left[\frac{|A|^2}{\mathcal{N}_0 + \mathcal{E}_s(1-(\rho^{l-1})^2)|A|^2}\right]} - 1 \right) \cdot \frac{1}{1-(\rho^{l-1})^2} \tag{2}$$

when

$$B^l(\omega) \propto \frac{A^*(\omega)}{\mathcal{N}_0 + \mathcal{E}_s(1-(\rho^{l-1})^2)|A(\omega)|^2} \tag{3}$$

$$D^l(\omega) = \rho^{l-1}\left(A(\omega)B^l(\omega) - E[AB^l]\right). \tag{4}$$

While the strictly causal feedback filter of the DFE subtracts out only postcursor ISI, the noncausal nature of the optimal $D^l(\omega)$ allows the iterated-decision equalizer to cancel both precursor and postcursor ISI. Moreover, the expression for the optimal $D^l(\omega)$ is intuitively satisfying. If $\hat{x}^{l-1}[n] = x[n]$ so that $\rho^{l-1} = 1$, then the output of $D^l(\omega)$ exactly reproduces the ISI component of $\tilde{r}^l[n]$. More generally though, the correlation coefficient ρ^{l-1} describes our confidence in the quality of the estimate $\hat{x}^{l-1}[n]$ and scales the ISI estimate accordingly. Note that the center tap of $d^l[n]$ is indeed zero, as stipulated earlier. Note also that during the first ($l = 1$) pass, the feedback branch is not used because $\rho^0 = 0$, so the sequence $\hat{x}^0[n]$ does not need to be defined.

Next, the properties of $v^l[n]$ imply that the probability of symbol error at the lth iteration is well-approximated by the high signal-to-noise ratio (SNR) formula for the M-ary PSK symbol error rate of a symbol-by-symbol threshold detector for additive white Gaussian noise (AWGN) channels, given by [7]

$$\Pr(\epsilon^l) = 2\mathcal{Q}\left(\sin\left(\frac{\pi}{M}\right)\sqrt{2\gamma^l}\right), \tag{5}$$

where $\mathcal{Q}(v) = \frac{1}{\sqrt{2\pi}}\int_v^\infty e^{-t^2/2}dt$.

By substituting (3) and (4) into (2) and exploiting the fact that arbitrarily close samples of the random process $A(\omega)$ are asymptotically independent in the limit as $L \to \infty$, it can be shown that

$$\gamma^l = \left(\frac{1}{\xi^l e^{\xi^l} E_1(\xi^l)} - 1\right) \cdot \frac{1}{1-(\rho^{l-1})^2} \tag{6}$$

where $E_1(s) = \int_s^\infty e^{-t}/t\ dt$ and $\xi^l = \zeta/(1-(\rho^{l-1})^2)$, with $1/\zeta = \mathcal{E}_s L\sigma_a^2/\mathcal{N}_0$ being the expected SNR at which the transmission is received.

As the above development suggests, successful implementation of the iterated-decision equalizer requires that the normalized correlation between the symbols $x[n]$ and $\hat{x}^{l-1}[n]$ at the lth pass be computable. The iterative algorithm for computing the set of correlation coefficients ρ^l, and in turn predicting the sequence of symbol error probabilities is as follows.

1. Set $\rho^0 = 0$ and let $l = 1$.
2. Compute the SINR γ^l at the slicer input on the lth decoding pass from ρ^{l-1} via (6). [It is worth pointing out that for shorter ISI channels, we can alternatively (and in some cases more accurately) compute γ^l from ρ^{l-1} via (2), where the expectation is replaced by a frequency average.]
3. Compute the symbol error probability $\Pr(\epsilon^l)$ at the slicer output from γ^l via (5).

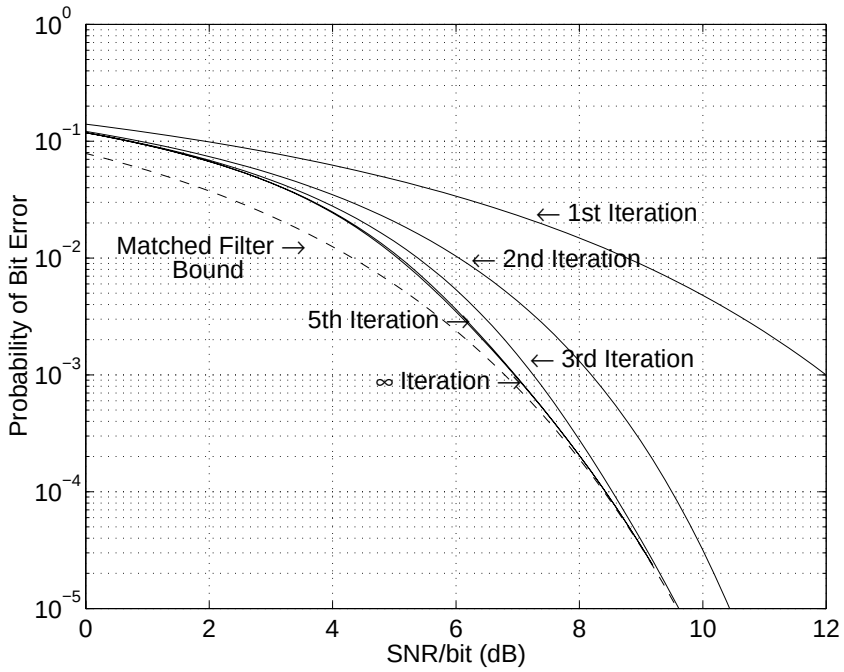

Figure 2: Theoretical QPSK bit-error rate for the iterated-decision equalizer as a function of SNR per bit and the number of decoding iterations.

4. Compute the normalized correlation coefficient ρ^l between the symbols $x[n]$ and the decisions $\hat{x}^l[n]$ generated at the slicer via [6]

$$\rho^l = 1 - 2\sin^2\left(\frac{\pi}{M}\right)\Pr(\epsilon^l). \tag{7}$$

5. Increment l and go to step 2.

A straightforward analysis of the algorithm reveals that the sequence of error probabilities $\Pr(\epsilon^1), \Pr(\epsilon^2), \ldots$ is monotonically decreasing, suggesting that additional iterations always improve performance. However, the error rate performance for a given SNR of $1/\zeta$ eventually converges to a steady-state value of $\Pr(\epsilon^\infty)$.

In Fig. 2, bit error rate is plotted as a function of SNR for $1, 2, 3, 5$, and an infinite number of iterations. We observe that steady-state performance is approximately achieved with comparatively few iterations, after which additional iterations provide only negligibly small gains in performance. It is significant that few passes are required to converge to typical target bit-error rates, since the amount of computation is directly proportional to the number of passes required. We emphasize that the complexity of the iterated-decision equalizer is comparable to that of the DFE or the LE. It is also significant to note that as the SNR increases ($\zeta \to 0$), the slicer input SINR $\gamma \to 1/\zeta$ which, when substituted into (5), corresponds to the matched filter bound for the channel. Thus, perfect ISI cancellation is approached at high SNR.

We plot in Fig. 3 the theoretical performance of the iterated-decision equalizer and the ideal minimum mean-square error decision-feedback equalizer (MMSE-DFE) as $L \to \infty$ [4], as well as the associated experimental performance when $L = 256$. We can readily see that at moderate to high SNR, the iterated-decision equalizer requires significantly less transmit power than the MMSE-DFE to achieve the same error rate. In fact, at high SNR, the iterated-decision equalizer theoretically requires $10\Gamma_0 \log e \approx 2.507$ dB

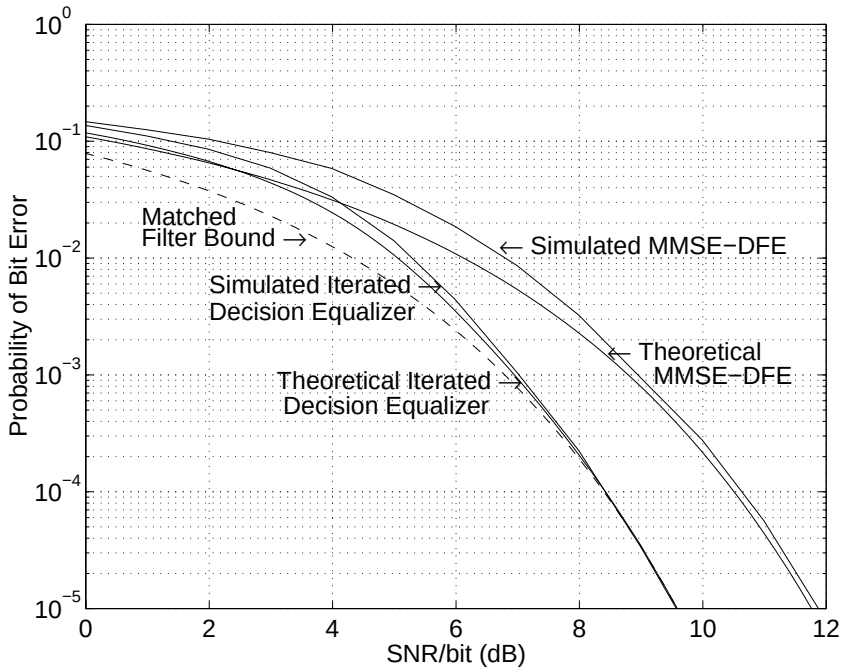

Figure 3: Theoretical and experimentally observed QPSK bit-error rate for the iterated-decision equalizer and the MMSE-DFE as a function of SNR per bit.

less transmit power [4] to achieve the same probability of error as the ideal MMSE-DFE, where $\Gamma_0 = 0.57721\cdots$ denotes Euler's constant.

2.1 Adaptive Implementations

We now develop an adaptive implementation of the iterated-decision equalizer, in which optimal FIR filter coefficients are selected automatically (from the received data) without explicit knowledge of the channel characteristics. We focus on the single channel case; multichannel generalizations follow in a straightforward manner, as developed in [4].

The iterated-decision equalizer is designed to process received data in a block-iterative fashion, so it is ideally suited for packet communication in which the packet size is chosen small enough that the channel encountered by each packet appears linear time-invariant. As is typically the case with other adaptive equalizers, the adaptive iterated-decision equalizer makes use of training symbols sent along in the packet with the data symbols. Suppose that a block of white M-ary PSK symbols $x[n]$ for $n = 0, 1, \ldots, N-1$ is transmitted; some of the symbols (not necessarily at the head of the packet) are for training, while the rest are data symbols.

In the adaptive implementation of the iterated-decision equalizer, the filters $b^l[n]$ and $d^l[n]$ for the lth iteration are finite-length filters. Specifically, $b^l[n]$ has J_1 strictly anticausal taps and J_2 strictly causal taps plus a center tap, while $d^l[n]$ has K_1 strictly anticausal taps and K_2 strictly causal taps with no center tap.

Before the first pass ($l = 1$), we need to initialize the hard decisions $\hat{x}^0[n]$. Since the locations and values of the training symbols in $x[n]$ are known at the receiver, we set $\hat{x}^0[n] = x[n]$ for the n corresponding to those locations. For all the other n between 0 and $N-1$ inclusive, we set $\hat{x}^0[n]$ to be a "neutral" value—for white PSK symbols, this value should be zero.

On the lth pass of the equalizer where $l = 1, 2, 3, \ldots$, the slicer input $\tilde{x}^l[n]$ can be expressed as[3]

$$\tilde{x}^l[n] = \mathbf{c}^{l\dagger}\mathbf{q}^l[n] \tag{8}$$

where

$$\mathbf{c}^{l\dagger} = \left[\begin{array}{cccccccccc} b^l[-J_1] & \cdots & b^l[0] & \cdots & b^l[J_2] & d^l[-K_1] & \cdots & d^l[-1] & d^l[1] & \cdots & d^l[K_2] \end{array}\right] \tag{9}$$

$$\mathbf{q}^l[n] = \left[\begin{array}{cccccccccc} r[n+J_1] & \cdots & r[n] & \cdots & r[n-J_2] & \hat{x}^{l-1}[n+K_1] & \cdots & \hat{x}^{l-1}[n+1] & \hat{x}^{l-1}[n-1] & \cdots & \hat{x}^{l-1}[n-K_2] \end{array}\right]^T. \tag{10}$$

Using a minimum-distance rule, the slicer then generates the hard decisions $\hat{x}^l[n]$ from $\tilde{x}^l[n]$ for all n between 0 and $N-1$ inclusive, except for those n corresponding to the locations of training symbols in $x[n]$. For those n, we set $\hat{x}^l[n] = x[n]$.

In the lth iteration, there are two sets of data available to the receiver: $r[n]$ and $\hat{x}^{l-1}[n]$, $n = 0, 1, \ldots, N-1$. If we assume that $x[n] \approx \hat{x}^{l-1}[n]$ for the purposes of determining the optimal filters (as is similarly done in the adaptive DFE in decision-directed mode), then it is reasonable to choose $b^l[n]$ and $d^l[n]$ so as to minimize the sum of error squares:

$$\mathcal{E}(\mathbf{c}^l) = \sum_{n=-\infty}^{\infty} |\hat{x}^{l-1}[n] - \mathbf{c}^{l\dagger}\mathbf{q}^l[n]|^2. \tag{11}$$

Since this is a linear least-squares estimation problem, the optimum $\mathbf{c}^l$ is [8]

$$\mathbf{c}^l_{\text{opt}} = [\mathbf{\Phi}^l]^{-1}\mathbf{u}^l, \tag{12}$$

where $\mathbf{\Phi}^l = \sum_{n=-\infty}^{\infty} \mathbf{q}^l[n]\mathbf{q}^{l\dagger}[n]$ and $\mathbf{u}^l = \sum_{n=-\infty}^{\infty} \hat{x}^{l-1^*}[n]\mathbf{q}^l[n]$. The resulting equalizer lends itself readily to practical implementation, even for large filter lengths. In particular, the matrix $\mathbf{\Phi}^l$ can be efficiently computed using correlation functions involving $r[n]$ and $\hat{x}^{l-1}[n]$, and $[\mathbf{\Phi}^l]^{-1}$ can be efficiently computed using formulas for the inversion of a partitioned matrix [9].

We now turn to a couple of implementation issues. First, we would ideally like our finite-length adaptive filters to approximate (3) and (4), which are infinite length. The optimal $b^l[n]$ in (3) includes a filter matched to $a[n]$, and the optimal $d^l[n]$ in (4) includes a cascade of $a[n]$ and the corresponding matched filter, suggesting that a reasonable rule of thumb is to select $J_1 = J_2 = K_1 = K_2 = L$. Second, the block-iterative nature of the equalizer allows the training symbols to be located anywhere in the packet. Since—in contrast to the DFE—the locations do not appear to affect equalizer performance, we arbitrarily choose to uniformly space the training symbols within each packet.

In Fig. 4, we plot the bit-error rate of the adaptive iterated-decision equalizer as a function of the number of iterations, for varying amounts of training data. The graph strongly suggests that there is a threshold for the number of training symbols, below which the adaptive equalizer performs poorly and above which the bit-error rate consistently converges to approximately the same steady-state value regardless of the exact number of training symbols. The excess training data is still important though, since the bit-error rate converges quicker with more training data.

We next examine the probability of bit error as a function of SNR for varying amounts of training data. From Fig. 5 we see that, as expected, performance improves as the amount of training data is increased. Moreover, only a modest amount of training symbols

[3]The superscripts ^{T} and † denote the transpose and conjugate-transpose operations, respectively.

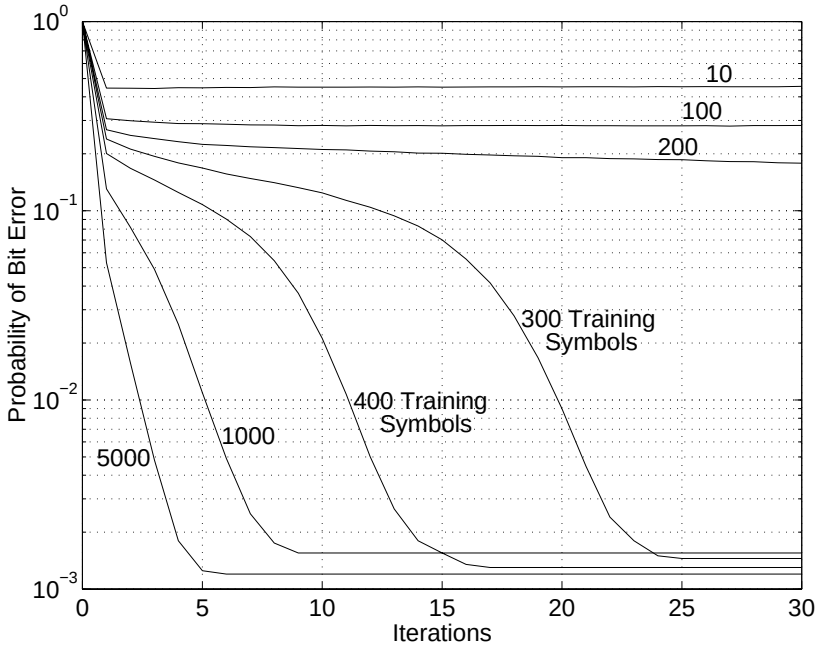

Figure 4: Experimentally observed QPSK bit-error rate for the adaptive iterated-decision equalizer as a function of the number of decoding iterations and the number of training symbols transmitted with each block of 10000 data symbols at an SNR per bit of 7 dB. The 100-tap channels were equalized using 201 feedforward taps and 200 feedback taps.

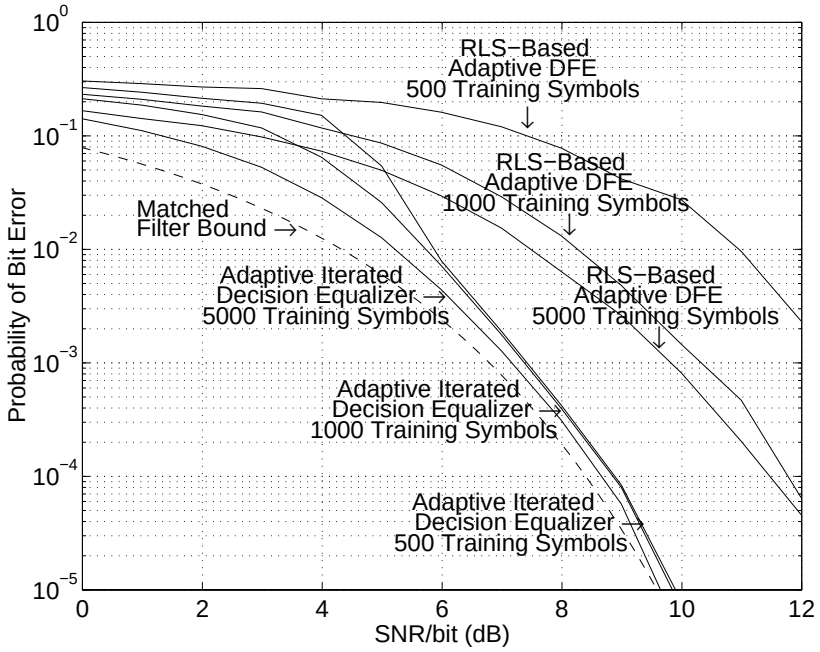

Figure 5: Experimentally observed QPSK bit-error rate for the adaptive iterated-decision equalizer and the RLS-based adaptive DFE (with forgetting factor $\lambda = 1$) as a function of SNR per bit. Blocks of 10000 data symbols were transmitted through 128-tap channels, which were equalized using 257 feedforward taps and 256 noncausal feedback taps in the case of the iterated-decision equalizer, and using 257 feedforward taps and 128 strictly causal feedback taps in the case of the DFE.

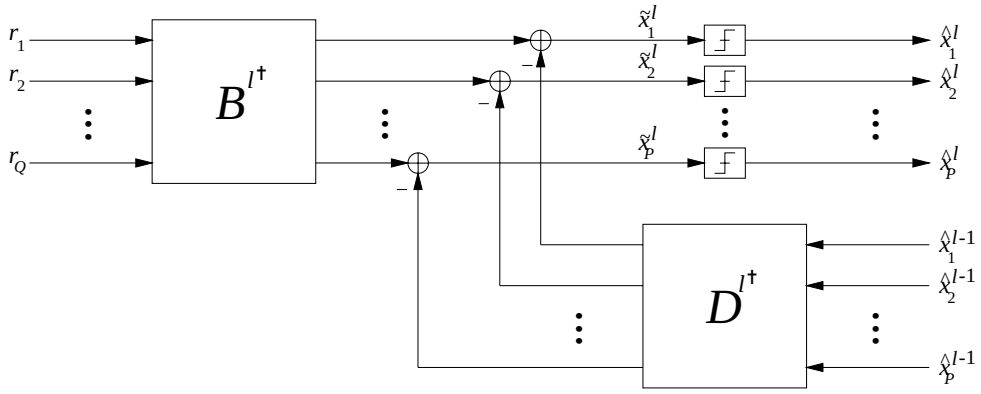

Figure 6: Multiuser iterated-decision detector structure.

is required at high SNR for the adaptive equalizer to perform as if the channel were exactly known at the receiver.

For comparison purposes, we also plot in Fig. 5 the performance of the recursive least squares (RLS) based implementation of the adaptive DFE [8]. The DFE performs significantly worse than the iterated-decision equalizer for comparable amounts of training data. Indeed, the high SNR gap is even larger than the 2.507 dB determined for the nonadaptive case. This is because, as Figs. 3 and 5 show, the performance of the adaptive DFE is not accurately predicted by the nonadaptive MMSE-DFE, even in the long ISI limit. It is also worth stressing that the RLS-based adaptive DFE is much more computationally expensive than the adaptive iterated-decision equalizer because the RLS-based DFE requires the multiplication of large matrices for *each* transmitted symbol, whereas the iterated-decision equalizer essentially requires the computation of one large matrix inverse per iteration for *all* the symbols in the packets, with the number of required iterations being typically small.

3 The Iterated-Decision Multiuser Detector

We now develop the counterpart of the iterated-decision equalizer for the multiuser detection problem.

For the purposes of illustration, we consider a P-user discrete-time synchronous channel model, where the ith user modulates an M-ary PSK symbol x_i onto a randomly generated signature sequence $\mathbf{h}_i = [\ h_i[1] \quad h_i[2] \quad \cdots \quad h_i[Q]\ ]^T$ of length Q assigned to that user, where the taps of the sequence are mutually independent, zero-mean, complex-valued, circularly symmetric Gaussian random variables with variance $1/Q$. The received signal is $\mathbf{r} = \mathbf{HAx} + \mathbf{w}$, where $\mathbf{H} = [\mathbf{h}_1|\cdots|\mathbf{h}_P]$ is the $Q \times P$ matrix of signatures, $\mathbf{A} = \mathrm{diag}\{A_1, \ldots, A_P\}$ is the diagonal matrix of received amplitudes, $\mathbf{x} = [\ x_1 \quad x_2 \quad \cdots \quad x_P\ ]^T$, and $\mathbf{w}$ is a Q-dimensional Gaussian vector with independent zero-mean, complex-valued, circularly symmetric components of variance $\mathcal{N}_0$.

The structure of the multiuser iterated-decision detector is depicted in Fig. 6. The vector of slicer inputs at each iteration is $\tilde{\mathbf{x}}^l = \mathbf{B}^{l\dagger}\mathbf{r} - \mathbf{D}^{l\dagger}\hat{\mathbf{x}}^{l-1}$, where $\mathbf{B}^l = [\mathbf{b}_1^l|\cdots|\mathbf{b}_P^l]$, $\mathbf{D}^l = [\mathbf{d}_1^l|\cdots|\mathbf{d}_P^l]$, and $\hat{\mathbf{x}}^{l-1} = [\ \hat{x}_1^{l-1} \quad \hat{x}_2^{l-1} \quad \cdots \quad \hat{x}_P^{l-1}\ ]^T$. Analogous to (1) in the case of equalization, the slicer input for the ith user at the lth iteration can be approximated as

$$\tilde{x}_i^l \approx A_i E[\mathbf{b}_i^{l\dagger}\mathbf{h}_i]x_i + v_i^l \tag{13}$$

with $v_1^l, v_2^l, \ldots, v_P^l$ as mutually uncorrelated, zero-mean, complex-valued, circularly symmetric Gaussian random variables, and where the accuracy of the approximation increases when the number of users P gets large while the ratio $\beta \stackrel{\triangle}{=} P/Q$ is held constant. If $\mathbf{I}_P$ and $\mathbf{I}_Q$ are the $P \times P$ and $Q \times Q$ identity matrices respectively, and if $E[x_i^* \cdot \hat{x}_j^{l-1}]/\mathcal{E}_s \approx \rho_i^{l-1}\delta[i-j]$ with $\boldsymbol{\rho}^{l-1} = \mathrm{diag}\{\rho_1^{l-1}, \ldots, \rho_P^{l-1}\}$, then the SINR at the slicer input for the ith user during the lth pass, i.e.,

$$\gamma_i^l = \frac{\mathcal{E}_s A_i E[\mathbf{b}_i^{l\dagger}\mathbf{h}_i]}{\mathrm{var}\ v_i^l} \tag{14}$$

achieves its maximum value when[4]

$$\mathbf{B}^l \ \propto \ \left[\mathcal{N}_0\mathbf{I}_Q + \mathcal{E}_s\mathbf{H}\mathbf{A}(\mathbf{I}_P - \boldsymbol{\rho}^{l-1}\boldsymbol{\rho}^{l-1^\dagger})\mathbf{A}^\dagger\mathbf{H}^\dagger\right]^{-1}\mathbf{H}\mathbf{A} \tag{15}$$

$$\mathbf{D}^l \ = \ \boldsymbol{\rho}^{l-1^\dagger}\left[\mathbf{A}^\dagger\mathbf{H}^\dagger\mathbf{B}^l - \mathrm{diag}\left\{(\mathbf{A}^\dagger E\left[\mathbf{H}^\dagger\mathbf{B}^l\right])_{11}, \ \ldots, (\mathbf{A}^\dagger E\left[\mathbf{H}^\dagger\mathbf{B}^l\right])_{PP}\right\}\right]. \tag{16}$$

In the case of accurate power control, i.e., $\mathbf{A} = A\mathbf{I}_P$ so $\boldsymbol{\rho}^{l-1} = \rho^{l-1}\mathbf{I}_P$, it can be shown that in the limit of large P, the SINR in (14) for each user achieved by these optimum choices of $\mathbf{B}^l$ and $\mathbf{D}^l$ is given by

$$\gamma^l = \left(\frac{1}{1 - \frac{1}{4\beta}\cdot\frac{\mathcal{N}_0}{\mathcal{E}_s(1-|\rho^{l-1}|^2)|A|^2}\cdot\mathcal{F}\left(\frac{\mathcal{E}_s(1-|\rho^{l-1}|^2)|A|^2}{\mathcal{N}_0}, \beta\right)} - 1\right)\cdot\frac{1}{1-(\rho^{l-1})^2} \tag{17}$$

where

$$\mathcal{F}(y,z) \stackrel{\triangle}{=} \left(\sqrt{y(1+\sqrt{z})^2+1} - \sqrt{y(1-\sqrt{z})^2+1}\right)^2. \tag{18}$$

The iterative algorithm for computing the correlation coefficients ρ^l, and in turn predicting the sequence of symbol error probabilities is as follows.

1. Set $\rho^0 = 0$ and let $l = 1$.
2. Compute the SINR γ^l from ρ^{l-1} via (17).
3. Compute the symbol error probability $\Pr(\epsilon^l)$ from γ^l via (5).
4. Compute ρ^l via (7).
5. Increment l and go to step 2.

In Fig. 7, we compare the bit-error rate of the multiuser iterated-decision detector with the bit-error rates of various other multiuser detectors as a function of SNR, when decoding $P = 128$ simultaneous users with signatures of length $Q = 128$ with power control. The multiuser iterated-decision detector significantly outperforms the other detectors at moderate to high SNR, and asymptotically approaches the matched filter bound for the single-user channel. Thus, perfect MAI cancellation is approached at high SNR.

[4]Using a matrix identity, $\mathbf{B}^l$ can alternatively be computed as

$$\mathbf{B}^l \propto \mathbf{H}\mathbf{A}\left[\mathcal{N}_0\mathbf{I}_P + \mathcal{E}_s(\mathbf{I}_P - \boldsymbol{\rho}^{l-1}\boldsymbol{\rho}^{l-1^\dagger})\mathbf{A}^\dagger\mathbf{H}^\dagger\mathbf{H}\mathbf{A}\right]^{-1},$$

which may be easier to evaluate depending on relative sizes of P and Q.

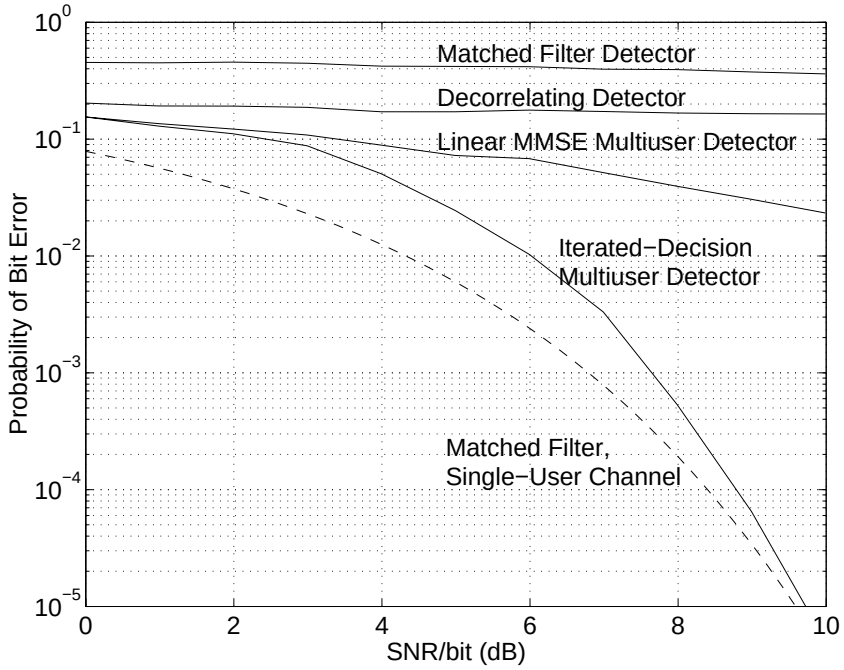

Figure 7: Experimentally observed QPSK bit-error rate for the multiuser iterated-decision detector and various other multiuser detectors as a function of SNR per bit. The number of simultaneous users is 128, and the signature length is 128.

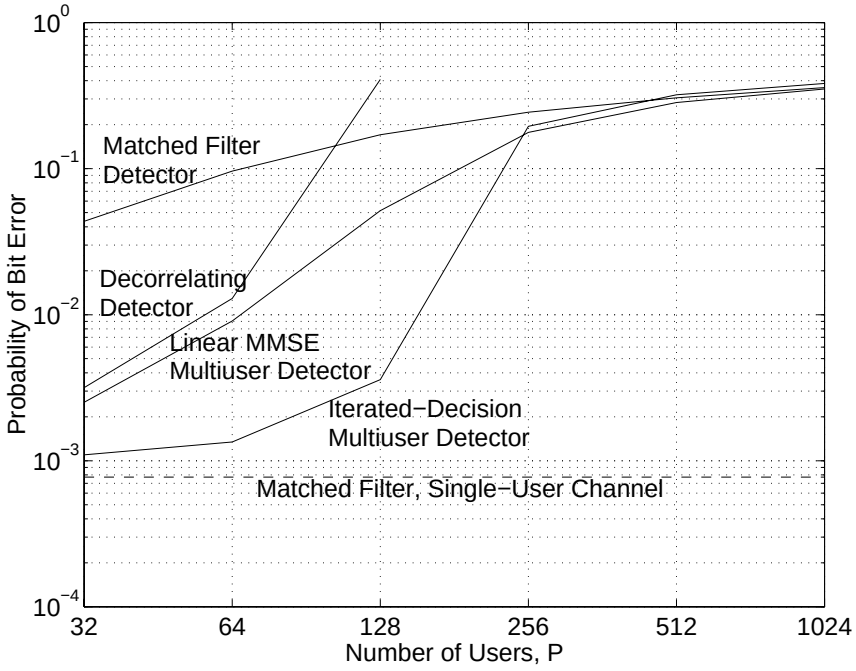

Figure 8: Experimentally observed QPSK bit-error rate for the multiuser iterated-decision detector and various other multiuser detectors as a function of the number of simultaneous users. The signature length is 128, and the SNR per bit is 7 dB.

Fig. 8 depicts the bit-error rates of the detectors as a function of the number of users P with signatures of length $Q = 128$, an SNR per bit of 7 dB, and power control. The multiuser iterated-decision detector has clearly superior performance when $P \lesssim 2Q$.

As a final comment, we note that an adaptive implementation of the iterated-decision multiuser detector is straightforward to derive, and is directly analogous to the adaptive iterated-decision equalizer of Section 2.1. Likewise, for coded systems, an iterated-decision multiuser decoder is readily obtained, and takes a form analogous to the iterated-decision equalizer-decoder structure mentioned in Section 2.

References

[1] C. A. Belfiore and J. H. Park, Jr., "Decision-feedback equalization," *Proc. IEEE*, vol. 67, pp. 1143–1156, Aug. 1979.

[2] S. Verdú, *Multiuser Detection*. Cambridge, U.K.: Cambridge Univ. Press, 1998.

[3] A. M. Chan and G. W. Wornell, "A Class of Block-Iterative Equalizers for Intersymbol Interference Channels," in *Int. Conf. Commun.,* (New Orleans, LA), June 2000.

[4] A. M. Chan, "A class of batch-iterative methods for the equalization of intersymbol interference channels," S. M. thesis, M.I.T., Aug. 1999.

[5] G. W. Wornell and M. D. Trott, "Efficient signal processing techniques for exploiting transmit antenna diversity on fading channels," *IEEE Trans. Signal Processing*, vol. 45, pp. 191–205, Jan. 1997.

[6] S. Beheshti, S. H. Isabelle, and G. W. Wornell, "Joint intersymbol and multiple-access interference suppression algorithms for CDMA systems," *European Trans. Telecomm. & Related Technol.*, vol. 9, pp. 403–18, Sep.–Oct. 1998.

[7] J. G. Proakis, *Digital Communications*, 3rd ed. New York: McGraw-Hill, 1995.

[8] S. Haykin, *Adaptive Filter Theory*, 3rd ed. Englewood Cliffs, NJ: Prentice Hall, 1996.

[9] H. Lütkepohl, *Handbook of Matrices*. Chichester, England: Wiley, 1996.

[10] E. Biglieri, "Ungerboeck codes do not shape the signal power spectrum," *IEEE Trans. Inform. Theory*, vol. 32, pp. 595–596, July 1986.